Supporting Information

Baruscotti et al. 10.1073/pnas.1010122108

SI Materials and Methods

Methods for Cardiac Telemetry. ECG telemetric recordings were performed with radio frequency transmitters (TA10ETA-F20, Data Sciences International) implanted in adult mice (>60 d old) according to a previously published protocol (1). Briefly, the transmitter was inserted into the intraperitoneal cavity; the reference lead was fixed to the dorsal surface of the xiphoid process and the recording lead was subcutaneously tunnelled in the thorax toward the upper insertion of the sternohyoid muscle and pushed under the muscle into the anterior mediastinum in a location close to the right atrium. During surgery the animals were anesthetized with 30 mg/kg tiletamine and 30 mg/kg zolazepam. After 1 wk of recovery, recording efficiency was tested in freely moving mice, and all telemetry experiments began 2 wk after the surgical positioning of the recording device. Cardiac rate was calculated from the RR duration (interval between two consecutive R waves of ECG, equivalent to cycle time). In an early set of experiments, the activity was recorded continuously and the rate was calculated by averaging data every 5 min. In later experiments, rate values were calculated as the mean of 5-min recordings collected every 30 min. To analyze the action of β-adrenergic receptor (β-AR) stimulation on rate, 0.1 mg/kg isoproterenol (Iso) was injected intraperitoneally in mice during telemetric recordings.

Sinoatrial Node Cell and Atrioventricular Node Cell Electrophysiology. Mice were deeply anesthetized by isofluoran and euthanized by cervical dislocation. Hearts were extracted, and the central sinoatrial node (SAN) and atrioventricular node (AVN) regions were isolated and used either for further enzymatic cell dissociation or for Western blot and immunolabeling analysis. Dissection of the AVN was performed according to previously published procedures (2).

Single SAN myocytes were obtained by enzymatic dissociation of SAN tissue as previously described (3); the same procedure was also used for the isolation of single AVN cells. The enzymatic solution contained collagenase IV (224 U/mL; Worthington), elastase (1.42 U/mL; Sigma-Aldrich), and protease (0.45 U/mL; Sigma-Aldrich). Isolated single cells were kept at 4 °C in Tyrode solution (mmol/L: NaCl, 140; KCl, 5.4; $CaCl_2$, 1.8; $MgCl_2$, 1; D-glucose, 5.5; Hepes-NaOH, 5; pH 7.4) for the day of the experiment and patch-clamp experiments were performed in the whole-cell configuration at 35 ± 0.5 °C. The pipette solution contained the following (mmol/L): K-Aspartate, 130; NaCl, 10; EGTA-KOH, 5; $CaCl_2$, 2; $MgCl_2$, 2; ATP (Na-salt), 2; creatine phosphate, 5; GTP (Na-salt), 0.1; pH 7.2.

The I_f current was recorded from single SAN/AVN cells superfused with Tyrode solution to which $BaCl_2$ (1 mmol/L) and $MnCl_2$ (2 mmol/L) were added to improve I_f dissection over other ionic components. To obtain current densities, currents were measured during steps to the range −55/−125 mV and −65/−125 mV in SAN and AVN cells, respectively, and normalized to cell capacitance. Activation curves of the SAN I_f currents were obtained by applying two-step protocols with a first step to a test voltage in the range −35/−135 mV and a second step to −120 mV. Test step durations varied from 10 s at −35 mV to 7.5 s at −135 mV to allow full current activation at each voltage. After normalization to maximum amplitude, tails currents measured at −120 mV were plotted to obtain the activation variable and averaged. Mean data points were fitted with the Boltzmann distribution: $y = 1/(1+\exp((V-V_{1/2})/s))$, where V is voltage, y fractional activation, $V_{1/2}$ the half-activation voltage, and s the inverse-slope factor. Activation time constants were calculated by fitting current traces during steps to the range −75/−125 mV from the holding potential of −35 mV with single exponential curves (4–6). Shifts of the I_f-activation curve induced by isoprenaline (1 μM) were obtained with a previously published protocol (7).

Action potentials were recorded from spontaneously beating SAN myocytes or small agglomerates of pacing cells (two to five cells) superfused with normal Tyrode solution, and the rate was measured with customized software as described previously (8). The action of β-AR stimulation on rate was evaluated during perfusion with 1 μM Iso. ciHCN4-KO mice used to evaluate the effect of Iso on I_f and the rate in single cells were euthanized at an advanced stage of the tamoxifen (Tam) procedure (day 4 to day 5) to maximize the effects of tamoxifen.

Western Blot and Immunofluorescence. For Western blot analysis (Fig. 4*F*), intact SANs were extracted from control or ciHCN4-KO mice, homogenized in a buffer solution (mmol/L: $Na_4P_2O_7$, 20; $NaPHO_4$, 20; $MgCl_2$, 1; EDTA, 0.5; sucrose, 300; protease inhibitors mix, pH 7.4) and centrifuged at 200 × *g* for 2 min at 4 °C. The pellet was discarded and the concentration of the proteins in the supernatant was measured by a colorimetric method (Bio-Rad DC protein assay). The protein extract was then diluted in lithium dodecyl sulfate (LDS) sample buffer (Invitrogen), warmed for 8 min at 70 °C, and loaded (30 μg/lane) on 4–12% NuPAGE gel (Invitrogen). Blotted proteins were exposed to blocking solution (mmol/L: NaCl 100; NaH_2PO_4 20, Na_2HPO_4 80, Tween-20 0.1%; nonfat dried milk 5%; pH 7.5) and incubated with the primary rabbit anti-HCN4 (Alomone Labs) and mouse anti-Cav3 (BD Bioscience) antibodies. Antibodies were diluted 1:200 (anti-HCN4) and 1:1,000 (anti-Cav3) in the same blocking solution. Secondary antibodies conjugated to horseradish peroxidase (Molecular Probes) were used at 1:5,000 dilution and visually detected by chemiluminescence (Immobilon Western, Millipore). Immunofluorescence analysis of tissue sections and single cells were performed according to previously published procedures (9) with minor adjustments. For tissue sections (Fig. 4*E* and Fig. S2), excised SAN preparations from mice were frozen in isopentane at −50 °C and stored at −80 °C until used for cryosectioning. Sections were then cut perpendicularly to the crista terminalis and allowed to rest at room temperature (RT) for 1 h. Sections were then rinsed in PBS and fixed in a 4% paraformaldehyde solution (10 min) at 4 °C. Another 20-min wash in PBS plus 0.1 M glycine was carried out before the permeabilization step with 0.3% Triton X-100 in PBS (30 min) and block with 10% normal donkey serum diluted in PBS containing BSA 1% and Triton X-100 0.1% (1 h at RT). Sections were incubated overnight at 4 °C with the following antibodies: primary rabbit anti-HCN4, rabbit anti-HCN1, and rabbit anti-HCN2 (Alomone Labs; 1:100 in PBS; Fig. 4*E* and Fig. S2).

The sections were then washed in PBS (2 h) and exposed (1 h at RT) to the secondary antibody: 1:1,000 of AlexaFluor 488 donkey anti-rabbit (Invitrogen). Sections were then thoroughly rinsed again in PBS (2 h) and mounted with Vectashield Mounting Medium with DAPI (Vector Laboratories). Coverslips were sealed with nail polish before image acquisition with a video-confocal microscope (ViCO, Nikon). Isolated SAN and AVN cells were plated on glass slides and fixed in 4% paraformaldehyde (8 min at 4 °C). Glass slides were rinsed with PBS containing 0.1 M glycine (20 min). Cells were then incubated (30 min) with PBS solution containing 0.3% Triton X-100, 1% BSA, and 10% donkey serum (Sigma) to induce permeabilization and block. Primary and secondary antibodies were diluted in PBS solution. Incubation (1:100) with the primary anti-HCN4 antibody (Alomone Labs) was carried out overnight at 4 °C. Cells were then thoroughly rinsed in PBS solu-

tion before exposure (1 h at RT) to the secondary antibody (1:1,000 of AlexaFluor 488 donkey anti-rabbit; Invitrogen). Finally, cells were washed for 30 min in PBS solution before mounting with Vectashield mounting medium with DAPI (Vector Laboratories). Representative labeling of SAN and AVN single cells from control and ciHCN4-KO mice at the fifth day of Tam treatment are shown in Figs. S1 and S3, respectively.

CHO cells were transiently transfected with 2.0 μg of mHCN1 and mHCN2 plasmids, and a procedure similar to that used for single-myocyte staining was adopted for control immunolabeling experiments with rabbit anti-HCN1 and rabbit anti-HCN2 (Alomone Labs; Fig. S2).

Control Mice: Genotypes and Treatments. $Hcn4^{lox/lox;Cre}$ mice were paired with sex- and age-matched $Hcn4^{lox/lox}$ littermates throughout the experimental analysis. Control experiments were also performed with mice of wild-type ($Hcn4^{+/+}$) and MerCreMer (MCM) genotypes or by injecting $Hcn4^{lox/lox;Cre}$ mice with vehicle alone. Because experimental data collected from the various control animals were not significantly different, when appropriate they were pooled together in the set of control data.

Cardiac Specificity of Cre Activation. The cardiac-specific activation of the Cre recombinase protein due to the presence of the α-myosin heavy chain (αMHC) promoter was verified by crossing MCM transgenic mice (10) with the reporter transgenic mouse line ROSA26-EYFP (11). For tissue section preparation, SAN, ventricle, brain, and skeletal muscle were isolated from MCM, ROSA26-EYFP mice 24 h after the fifth injection of tamoxifen. After the isolation, tissues were frozen in isopentane at −50 °C and stored at −80 °C until used for cryosectioning. Endogenous fluorescence of tissue slices (10 μm thick) was then evaluated with a fluorescence microscope. Positive signals could be detected only in the SAN and in the ventricle.

Efficacy of Tam Treatment. We ran a set of pilot experiments aimed to verify the efficacy of Tam treatment. As shown in *Results*, the Tam treatment yielded deep bradycardia in ciHCN4-KO mice. As well as bradycardia, which could be quantified only by telemetry, Tam-treated ciHCN4-KO mice progressively developed a set of visible somatic and behavioral features, the most remarkable being a reduced motor activity and a reduced reactivity to mild mechanical stimuli. We noted, however, that in a number of cases no signs of bradycardia (in mice subject to telemetry) or of any somatic/behavioral modifications were visible and that ciHCN4-KO mice exposed to Tam did not respond to the treatment. Nonresponders were found in ciHCN4-KO mice subject to telemetry (9 over 29) and in ciHCN4-KO mice treated with Tam for other experimental protocols (31 over 87). Nonresponders were not distinguishable from untreated or Tam-treated control mice. For example, electrophysiological analysis of SAN cells isolated from nonresponders showed no significant differences with control animals: the I_f current density at −125 mV was −46.0 ± 4.2 pA/pF (n = 14), and the rate of spontaneous activity was 410.6 ± 23.8 bpm (n = 9), relative to −49.2 ± 5.2 pA/pF (n = 42) and 422.0 ± 24.5 bpm (n = 12) in cells from control animals (both nonsignificantly different, $P > 0.05$). Mean heart rates measured by telemetry were also nonsignificantly different (491.7 ± 19.3 bpm in n = 4 nonresponders vs. 537.2 ± 19.0 bpm in n = 9 control mice, as measured at day 8.5 of Tam treatment; $P > 0.05$). These data imply that lack of response in these mice is attributable to occasional lack of efficiency of Tam-induced recombination. All data presented in this work refer to mice that responded to Tam treatment.

1. Sgoifo A, et al. (1996) Electrode positioning for reliable telemetry ECG recordings during social stress in unrestrained rats. *Physiol Behav* 60:1397–1401.
2. Marionneau C, et al. (2005) Specific pattern of ionic channel gene expression associated with pacemaker activity in the mouse heart. *J Physiol* 562:223–234.
3. DiFrancesco D, Ferroni A, Mazzanti M, Tromba C (1986) Properties of the hyperpolarizing-activated current (if) in cells isolated from the rabbit sino-atrial node. *J Physiol* 377:61–88.
4. Bucchi A, et al. (2006) Wild-type and mutant HCN channels in a tandem biological-electronic cardiac pacemaker. *Circulation* 114:992–999.
5. Qu J, et al. (2001) HCN2 overexpression in newborn and adult ventricular myocytes: Distinct effects on gating and excitability. *Circ Res* 89:E8–E14.
6. Altomare C, et al. (2001) Integrated allosteric model of voltage gating of HCN channels. *J Gen Physiol* 117:519–532.
7. Accili EA, DiFrancesco D (1996) Inhibition of the hyperpolarization-activated current (i_f) of rabbit SA node myocytes by niflumic acid. *Pflugers Arch* 431:757–762.
8. Bucchi A, Baruscotti M, Robinson RB, DiFrancesco D (2003) I(f)-dependent modulation of pacemaker rate mediated by cAMP in the presence of ryanodine in rabbit sino-atrial node cells. *J Mol Cell Cardiol* 35:905–913.
9. Brioschi C, et al. (2009) Distribution of the pacemaker HCN4 channel mRNA and protein in the rabbit sinoatrial node. *J Mol Cell Cardiol* 47:221–227.
10. Sohal DS, et al. (2001) Temporally regulated and tissue-specific gene manipulations in the adult and embryonic heart using a tamoxifen-inducible Cre protein. *Circ Res* 89: 20–25.
11. Srinivas S, et al. (2001) Cre reporter strains produced by targeted insertion of EYFP and ECFP into the ROSA26 locus. *BMC Dev Biol* 1:4.

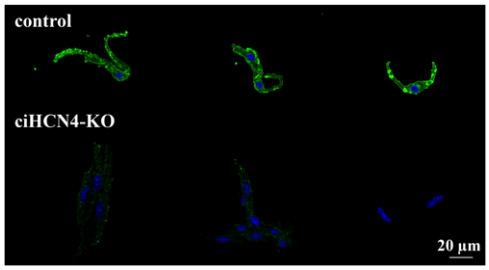

Fig. S1. HCN4 immunolabeling in SAN cells. Representative video-confocal images of cells isolated from the SAN of control (*Upper*) and ciHCN4-KO mice (*Lower*) immunolabeled with antibodies against the HCN4 protein. Both control and ciHCN4-KO mice received full Tam treatment before cell isolation. In control cells, the membrane-associated fluorescence is strong and characterized by a spot-like signal appearance typical of the distribution of HCN4 channels in pacemaker cells. Cells isolated from ciHCN4-KO mice display a much reduced fluorescence intensity. Nuclei are labeled with DAPI (blue).

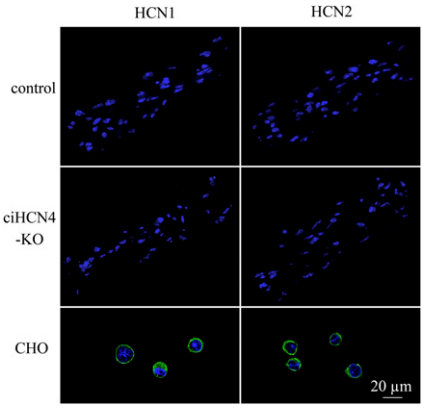

Fig. S2. Lack of detectable HCN1 and HCN2 protein expression in the SAN of control and ciHCN4-KO mice. HCN1 (*Left*) and HCN2 (*Right*) immunolabeling of the central portion of SAN slices yielded no detectable signals from either control (*Top*) or ciHCN4-KO mice (*Middle*). The functionality of both antibodies was verified by immunolabeling of CHO cells expressing the two channels (*Bottom*). Nuclei are labeled with DAPI (blue).

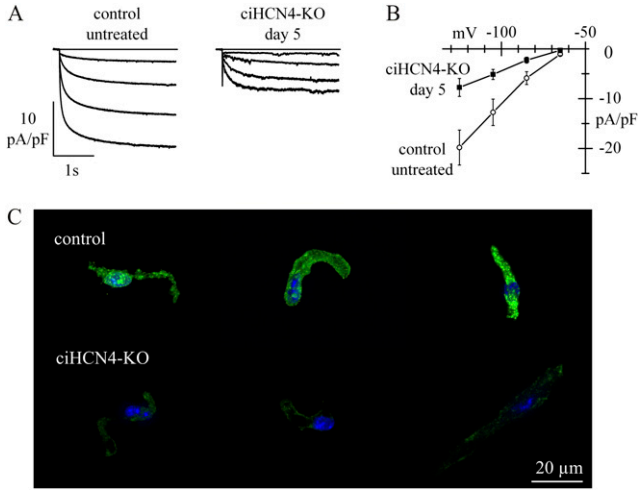

Fig. S3. I_f current and HCN4 expression in AVN cells. (*A*) Sample I_f current traces activated by hyperpolarizing steps to −65, −85, −105, and −125 mV from a holding potential of −35 mV in single cells isolated from the AVN region of control and ciHCN4-KO mice. (*B*) Mean steady-state current/voltage (I/V) curves recorded in cells isolated from control untreated mice (open circles, n = 7/3 cells/mice) and from ciHCN4-KO mice after 5 d of Tam treatment (solid squares, n = 7/2). Data points are significantly different at all potentials ($P < 0.05$). (*C*) Representative video-confocal images of cells isolated from the AVN of control untreated (*Upper*) and day 5 ciHCN4-KO mice (*Lower*) immunolabeled with anti-HCN4 antibody. Control cells are clearly labeled, while the signal from ciHCN4-KO cells is strongly reduced. Nuclei are labeled with DAPI (blue).

Table S1. Mean cell capacitance and mean I_f current densities

Mice	Capacitance (pF)	I_f density (pA/pF) At −55 mV	At −65 mV	At −85 mV	At −105 mV	At −125 mV
Control untreated	31.9 ± 1.4 (*n* = 44)	−2.2 ± 0.2 (*n* = 22)	−5.8 ± 0.6 (*n* = 44)	−20.4 ± 1.8 (*n* = 44)	−36.6 ± 3.1 (*n* = 44)	−50.4 ± 4.5 (*n* = 44)
Control day 5	30.8 ± 1.6 (*n* = 42)	−2.6 ± 0.4 (*n* = 22)	−5.1 ± 0.6 (*n* = 42)	−19.4 ± 2.1 (*n* = 42)	−35.5 ± 3.6 (*n* = 42)	−49.2 ± 5.2 (*n* = 42)
ciHCN4-KO day 2	30.1 ± 1.5 (*n* = 32)	−1.5 ± 0.4* (*n* = 22)	−3.5 ± 0.6* (*n* = 32)	−13.0 ± 1.6* (*n* = 32)	−23.2 ± 2.6* (*n* = 32)	−31.2 ± 3.6* (*n* = 32)
ciHCN4-KO day 5	31.4 ± 1.6 (*n* = 42)	−0.6 ± 0.1*,† (*n* = 30)	−1.6 ± 0.2*,† (*n* = 42)	−6.4 ± 0.7*,† (*n* = 42)	−11.7 ± 1.3*,† (*n* = 42)	−15.9 ± 1.8*,† (*n* = 42)

Control untreated and control day 5 means were nonsignificantly different in the entire voltage range investigated (*t* test, $P > 0.05$). No significant differences were found for cell capacitance.
*Significantly different from control according to one-way ANOVA followed by Fisher test (0.05 significance).
†Significantly different from ciHCN4 KO day 2 according to one-way ANOVA followed by Fisher test (0.05 significance).

Table S2. Mean Action Potential (AP) spontaneous rates

Mice	Rate (bpm)
Control	444.5 ± 23.7 (*n* = 15)
Control day 5	422.0 ± 24.5 (*n* = 12)
ciHCN4-KO day 2	293.6 ± 20.2* (*n* = 20)
ciHCN4-KO day 5	173.1 ± 21.6** (*n* = 26)

*$P < 0.05$ vs. control and control day 5; **$P < 0.05$ vs. control, control day 5 and ciHCN4-KO day 2.

Table S3. Mean heart rates

Mice	No. of mice	Basal rate (bpm)	+Iso 0.1 mg/Kg (bpm)
Control day 5	5	512.1 ± 20.2	705.0 ± 5.7*
ciHCN4-KO day 5	7	301.1 ± 12.0	485.8 ± 16.8*,†

*$P < 0.05$ vs. basal rate of matched group.
†$P < 0.05$ vs. rate in control in Iso.

Table S4. Mean spontaneous rates from isolated SAN cells

Mice	No. of cells	Tyrode solution (bpm)	+Iso 1 μM (bpm)
Control	10	376.0 ± 17.1	489.0 ± 8.4*
Control day 4/5	6	355.1 ± 10.2	475.0 ± 28.2*
ciHCN4-KO day 4/5	10	136.4 ± 15.4	279.9 ± 26.9*,†

*$P < 0.05$ vs. rate in Tyrode solution of matched group.
†$P < 0.05$ vs. rate in Iso in control and control day4/5.

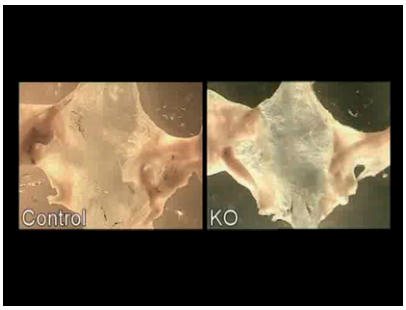

Movie S1. Spontaneous activity of whole SAN preparations extracted from a control mouse and a ciHCN4-KO mouse at day 5 of Tam treatment.

Movie S1

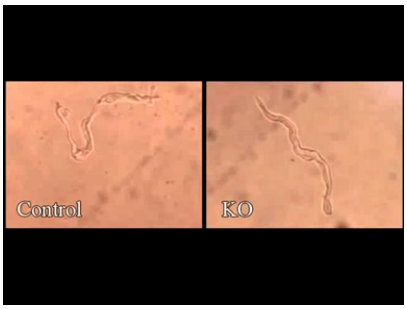

Movie S2. Spontaneous activity of single cells isolated from the SAN of a control mouse and a ciHCN4-KO mouse at day 5 of Tam treatment.

Movie S2